Reactive & Functional Polymers 73 (2013) 1180–1187

Contents lists available at SciVerse ScienceDirect

Reactive & Functional Polymers

journal homepage: www.elsevier.com/locate/react

Preparation of π-conjugated polymers consisting of 1-aminopyrrole and 4-amino-1,2,4-triazole units

Syusaku Koie, Gentaro Tanaka, Hiroki Fukumoto, Take-aki Koizumi, Takakazu Yamamoto *

Chemical Resources Laboratory, Tokyo Institute of Technology, 4259 Nagatsuta, Midori-ku, Yokohama 226-8503, Japan

ARTICLE INFO

Article history:
Received 30 January 2013
Received in revised form 23 May 2013
Accepted 26 May 2013
Available online 3 June 2013

Keywords:
π-Conjugated polymers
Poly(1-aminopyrrole)
4-Amino-1,2,4-triazole
BOC-protecting group
Organometallic polymerization

ABSTRACT

π-Conjugated polymers based on 1-aminopyrrole and 4-amino-1,2,4-triazole were prepared. Pd-catalyzed organometallic polycondensation gave poly(arylene-ethynylene) (PAE)-type π-conjugated polymers consisting of BOC-protected 4-amino-1,2,4-triazole (**Taz(BOC)**) units (BOC = *t*-butoxycarbonyl). The number average molecular weights (M_n) were determined to be 5200–19,200 using GPC. An alternating copolymer of **Taz(BOC)** and bithiophene (Th–Th) units, **P(Taz(BOC)-Th-Th)$_n$-Pd**, with an M_n of 10,800 was also prepared by Pd-catalyzed organometallic polycondensation. **(Taz(BOC)-Th-Th)$_n$-Pd** showed a UV–Vis absorption peak at λ_{max} = 425 nm, which is reasonable for a π-conjugated five-membered ring polymer with a coplanar structure. The deprotection of the BOC group of the polymers proceeded at 200 °C; this BOC-deprotection was investigated using a model compound. The optical and electrochemical properties of the π-conjugated polymers are reported.

1. Introduction

π-Conjugated 5-membered ring polymers have been the subject of many studies [1–7]. Polypyrroles have attracted the interest of many researchers. However, poly(1-aminopyrrole) with —NH_2 side groups has received less attention. Because the —NH_2 group is reactive, and can be converted into various functionalities, including nitro groups, imine groups, and diazonium groups, easy syntheses of polypyrrole with the —NH_2 side group have the potential to expand the scope of polypyrrole chemistry.

Losada and Armada [8] and Osaka et al. [9] reported the chemical and electrochemical oxidative (or dehydrogenative) polymerization of 1-aminopyrrole (cf. Scheme 1).

However, the obtained polymer was not well characterized. The presence of three reactive sites, i.e., the —NH_2 group and the 2- and 5-positions of the pyrrole ring, may complicate oxidative polymerization. Reactions at the 2- and 5-positions will result in the formation of a polypyrrole-type π-conjugated polymer. However, the presence of the reactive —NH_2 group may facilitate the introduction of a polyaniline-type junction (—NH-aromatic group-junction) into the polypyrrole-type π-conjugated structure.

We previously reported the oxidative polymerization of 1-aminopyrrole to π-conjugated polypyrrole-type polymers after the conversion of —NH_2 groups to —N=CHAr (Ar = aromatic group) groups [10]. We also reported the preparation of the BOC-protected monomers (**monomer-1** and **monomer-2**) shown in Scheme 2 [11], the oxidative polymerization of **monomer-1**, and the dehalogenative organometallic polymerization of **monomer-2**. Previously we focused on the syntheses of **monomer-1** and **monomer-2** and on the chemical and physical properties of the obtained polymers.

Recently, Yamaguchi and Asano reported the synthesis of a polypyrrole with viologen side chains from 1-aminopyrrole [12].

In this paper, we report the chemical and physical properties of **P1**-type polymers. In addition, we will be concerned with the expansion of our work on poly(1-aminopyrrole) to related polymers consisting of *4-amino-1,2,4-triazole* units. The new polymers were synthesized via the routes in Scheme 3. **Monomer-3**, a building block in these syntheses, was reported by our previous group [11].

The BOC-protecting group in both **P1** polymer the polymers shown in Scheme 3 is thought to be removed by thermal treatment [13–15]. The chemical properties of the —NH_2 bearing poly(1-aminopyrrole) and poly(4-amino-1,2,4-triazole) will also be reported.

As shown in Scheme 3, 4-amino-1,2,4-triazole polymers were prepared by Pd-catalyzed organometallic polycondensation. In addition to the organometallic polycondensation, the electrochemical oxidative polymerization of **monomer-7** was also attempted (cf. Scheme 4).

Because 4-amino-1,2,4-triazole contains electron-accepting imine —C=N— groups, it is not suited for electrochemical oxidative polymerization. However, the electrochemical oxidative polymerization of **monomer-7** which has electron-donating thiophene wings might be favorable.

---

* Corresponding author. Tel.: +81 45 924 5220; fax: +81 81 45 924 5976.
E-mail address: tyamamot@res.titech.ac.jp (T. Yamamoto).

1381-5148/$ - see front matter © 2013 Elsevier Ltd. All rights reserved.
http://dx.doi.org/10.1016/j.reactfunctpolym.2013.05.013

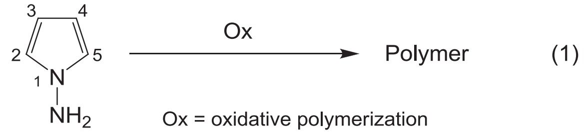

Scheme 1. Oxidative polymerization of 1-aminopyrrole via chemical oxidation with chloranil [8] and electrochemical oxidation [9].

4-Amino-1,2,4-triazole-based compounds have attracted the interest of materials scientists [16–18], particularly those working on organic magnets. Researchers in this field have conducted theoretical calculations of the electronic states of the π-conjugated homopolymers of 4-amino-1,2,4-triazole. However, good synthesis methods for 4-amino-1,2,4-triazole-based polymers have yet to be developed.

2. Experimental

2.1. Materials, general procedures, and measurements

Monomers-1, **-2**, and **-3** and **P1**-type polymers **P1-Ox** (cf. Scheme 2), with an M_n (number average molecular weight) and an M_w (weight average molecular weight) of 12,800 and 17,600, respectively [11], and **P1—Ni** (cf. Scheme 2) were prepared as reported previously [11]. **P1—Ni** showed an M_n and an M_w of 4,300 and 5,500 respectively from GPC (gel permeation chromatography; eluent = DMF; vs. polystyrene standards). A precursor of **monomer-7**, 2,5-bis(2-thienyl)-4-amino-1,2,4-triazole (**compound A**, a BOC-non-protected compound of **monomer-7**; cf. Scheme 5 shown below), was prepared according to the literature [19,20]. **Monomer-4** [21,22] and **monomer-5** [23,24], which were used in the preparation of **PAE**s (cf. Scheme 3), were prepared similarly

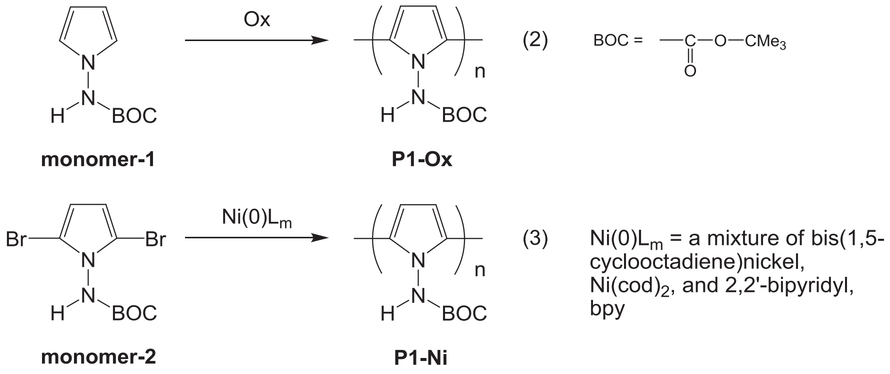

Scheme 2. Oxidative polymerization of BOC-protected 1-aminopyrrole (**monomer-1**; oxidizing reagent = $FeCl_3$) and organometallic polycondensation of 2,5-dibromo-1-aminopyrrole (**monomer-2**) using the zero-valent nickel complex $Ni(0)L_m$.

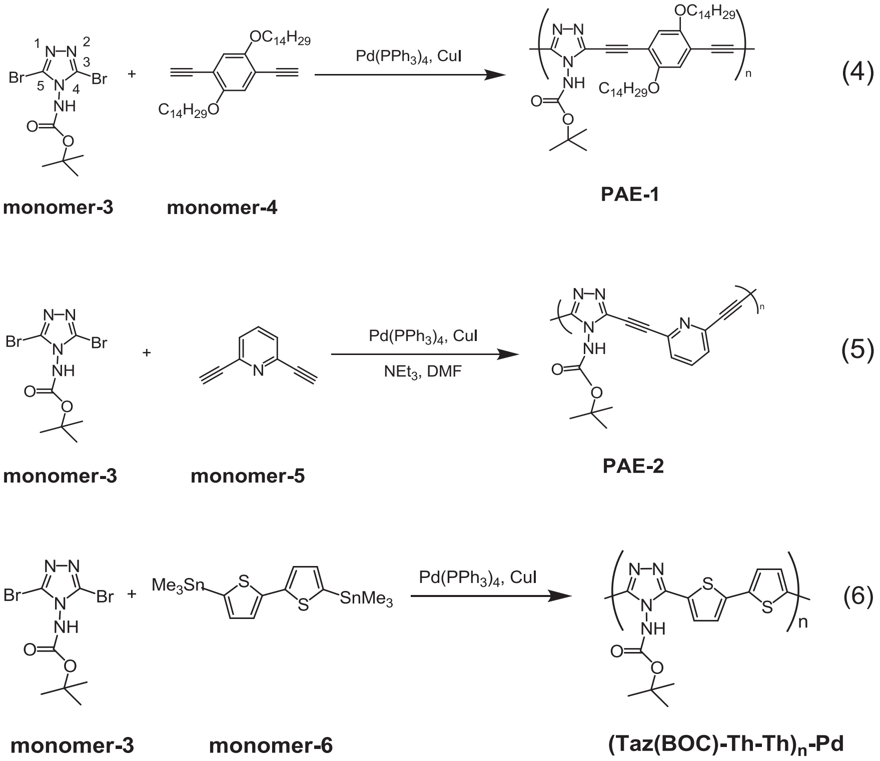

Scheme 3. Syntheses of polymers consisting of the 4-amino-1,2,4-triazole units. Poly(aryleneethynylene)s (**PAE**s) and an alternating copolymer, **$(Taz(BOC)\text{-}Th\text{-}Th)_n$-Pd**, consisting of a BOC-protected 4-amino-1,2,4-triazole (**Taz(BOC)**) unit via organometallic polycondensation.

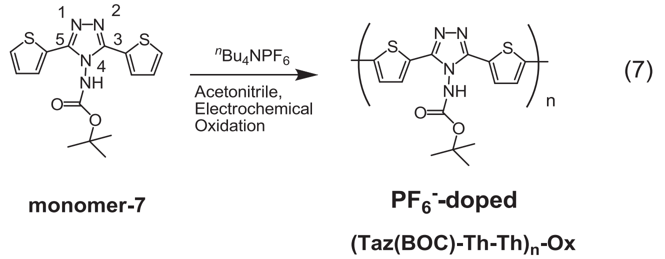

monomer-7

PF$_6^-$-doped (Taz(BOC)-Th-Th)$_n$-Ox

Scheme 4. Attempted electrochemical oxidative polymerization of **monomer-7**.

to previously reported methods. **Monomer-6** was used as received. Organometallic polymerization was conducted using standard Schlenk techniques.

IR spectra were measured with a JASCO IR-810 spectrometer. The ^{1}H and ^{13}C NMR spectra of the solution samples were recorded on a JEOL JNM-EX300, JEOL-LA300, or JEOL EX-400 spectrometer. The ^{13}C-CP/MAS NMR spectra of the solid samples were recorded on a JEOL JNM-ECA600 spectrometer. UV–Vis spectra were obtained with Shimadzu UV-3100PC and UV-2550 spectrometers. Thermogravimetric analyses (TGA) were conducted under N_2 with a Shimadzu TGA-50 and a TA-50WS. GPC analyses were performed using a Tosoh HLC-8120 analyzer (eluent = DMF containing LiBr) or a Shimadzu CTO-20 analyzer (eluent = chloroform) with polystyrene standards. Elemental analyses were conducted using a LECO CHNS-932 analyzer and a Yanako YS-10 SX-Elements microanalyzer at the Center for Advanced Materials Analysis (Suzukakedai), Technical Department, Tokyo Institute of Technology. Cyclic voltammetry (CV) was performed with a Hokuto HSV-100 or a BAS ALS 1200A.

2.2. Preparation of **monomer-7** and its related di-BOC compound, **compound B** (cf. Scheme 5)

A mixture of 3,5-bis(2-thienyl)-4-amino-1,2,4-triazole (**compound A**) [19,20] (2.00 g, 8.05 mmol), di-*t*-butyl dicarbonate ($(BOC)_2O$, 3.52 g, 16.1 mmol), and *N*,*N*-dimethyl-4-aminopyridine (DMAP, 1.97 g, 16.1 mmol) in 30 mL of dry *N*,*N*-dimethylformamide (DMF) was stirred for 6 h at 85 °C. This reaction mixture was poured into water, and a powder was separated by filtration and dissolved in chloroform. After filtration, the chloroform solution was condensed and washed with water three times. After the chloroform solution was dried over $MgSO_4$, it was poured into hexane to obtain a white powder. The powder was separated by filtration and dried under vacuum to obtain **monomer-7** (0.95 g, 34% yield). ^{1}H NMR (300 MHz, dimethyl sulfoxide (DMSO)-d_6) δ = 11.49 (s, major) and 10.95 (s, minor) (N*H* peaks for cis and trans rotamers in view of the —NH—CO— bond [11], 1H), 7.84 (dd, J = 4.8 Hz, 1.2 Hz, 2H), 7.68 (dd, J = 3.6 Hz, 1.2 Hz, 2H), 7.27 (dd, J = 4.8 Hz, 3.6 Hz, 2H), 1.45 (s, major) and 1.08 (s, minor) (C*H*$_3$ peaks for cis and trans rotamers in view of the —NH—CO-bond [11], 9H). IR (KBr, cm^{-1}): 1736 cm^{-1}. Anal. Calcd. for $C_{15}H_{16}N_4O_2S_2$: C, 51.70; H, 4.63; N, 16.08; S, 18.41%. Found: C, 51.54; H, 4.52; N, 16.32; S, 18.67%.

A similar reaction of **compound A** (300 mg, 1.21 mmol) with $(BOC)_2O$ (520 mg, 2.42 mmol) in dry THF (10 mL) in the presence of DMAP (250 mg, 2.0 mmol) was conducted for 5 h at 85 °C. After the removal of the solvent under vacuum, the residue was dissolved in chloroform. The product was purified on a basic Al_2O_3 column (eluent = 3:1 (v/v) mixture of chloroform and hexane) and recrystallized from ethyl acetate, giving white crystals of the di-BOC-protected **compound B** (120 mg, 22% yield). ^{1}H NMR (300 MHz, DMSO-d_6) δ = 7.92 (dd, J = 4.8 Hz, 1.2 Hz, 2H), 7.54 (dd, J = 3.6 Hz, 1.2 Hz, 2H), 7.31 (dd, J = 4.8 Hz, 3.6 Hz, 2H), 1.31 and 1.22 (s, 18H). Anal. Calcd. for $C_{20}H_{24}N_4O_4S_2$: C, 53.55; H, 5.39; N, 12.49; S, 14.30%. Found: C, 53.32; H, 5.41; N, 12.32; S, 14.55%.

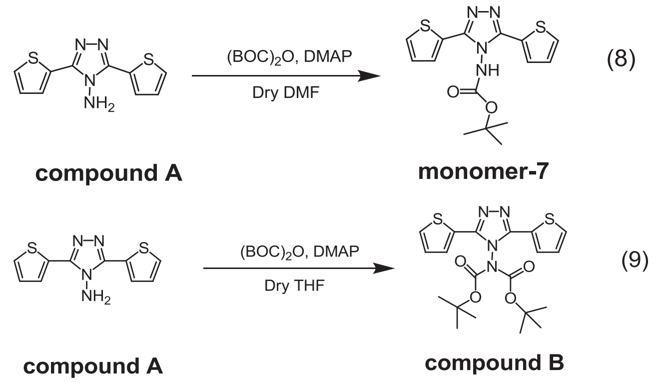

compound A

monomer-7

compound A

compound B

Scheme 5. Reactions of 3,5-bis(2-thienyl)-4-amino-1,2,4-triazole with $(BOC)_2O$ in DMF (Eq. (8)) and THF (Eq. (9)).

2.3. Preparation of new polymers

2.3.1. Poly(aryleneethynylene)s, **PAE-1** and **PAE-2**

The **PAE**s shown in Scheme 3 were prepared via the Pd-catalyzed couplings of **monomer-3** and diethynyl compounds [21–24].

A mixture of **monomer-3** (227 mg, 0.66 mmol), **monomer-4** (342 mg, 0.62 mmol), $Pd(PPh_3)_4$ (tetrakis(triphenylphosphine)palladium(0)), 38 mg, 0.03 mmol), CuI (10 mg, 0.05 mmol), dry DMF (20 mL), and N_2-purged triethylamine (10 mL) was stirred for 18 h at 60 °C. The reaction product was washed with methanol twice and dissolved in chloroform. After filtration, the chloroform solution was concentrated, and the polymer was recovered by reprecipitation in methanol. Drying under vacuum gave green **PAE-1** (167 mg, 35% yield). Some of the polymer was lost during work-up because of its good solubility. ^{1}H NMR (300 MHz, $CDCl_3$) δ = 7.2–6.7 (br, overlapped with residual protons in $CDCl_3$), ca. 4.0 (br, 4H), ca. 1.9 (br, 4H), 1.8–0.8 (59H). IR (KBr, cm^{-1}): 2212 (ν (C≡C)), 1745 (ν (C=O)) cm^{-1}, M_n = 19,200 M_w = 23,300. A dioctyloxy analogue of **PAE-1**, **PAE-3** (color: deep green), was obtained with a 93% yield via an analogous route using **monomer-3** (270 mg, 0.79 mmol) and a dioctyloxy analogue (301 mg, 0.79 mmol) of **monomer-4**. The characterization of this polymer was not performed because it was insoluble in the solvents tested.

A mixture of **monomer-3** (800 mg, 2.34 mmol), **monomer-5** (300 mg, 2.36 mmol), $Pd(PPh_3)_4$ (140 mg, 0.12 mmol), CuI (20 mg, 0.11 mmol), dry DMF (30 mL), and N_2-purged triethylamine (15 mL) was stirred for 14 h at 60 °C. The reaction mixture was poured into water, and the precipitate was separated by filtration. The solids were washed with acetone, methanol, and diethyl ether, and dried under vacuum to obtain **PAE-2** (270 mg, 36% yield). ^{1}H NMR (300 MHz, DMSO-d_6) δ = 7.92 (br, 2H, pyridine-3,5-Hs), 7.39 (br, 1H, pyridine-4-H), 1.56–1.04 (9H, —C*H*$_3$). IR (KBr, cm^{-1}): 2209 (ν (C≡C)), 1742 (ν (C=O)) cm^{-1}, M_n = 5,200 M_w = 7,100.

2.3.2. **(Taz(BOC)-Th-Th)$_n$-Pd** and electrochemical oxidation of **monomer-7**

The Stille-type polycondensation of **monomer-3** and **monomer-6** using $Pd(PPh_3)_4$ as the catalyst [2] gave **(Taz(BOC)-Th-Th)$_n$-Pd** (Scheme 3).

A mixture of **monomer-3** (1.37 g, 4.0 mmol), **monomer-6**, (1.97 g, 4.0 mmol), $Pd(PPh_3)_4$ (470 mg, 0.4 mmol), CuI (80 mg, 0.4 mmol), and dry DMF (40 mL) was stirred for 168 h at 80 °C. The reaction mixture was poured into an aqueous solution of KF, and the precipitate was collected by filtration. The solids were washed with aqueous ammonia, an aqueous solution of the disodium salt of ethylenediaminetetraacetic acid EDTA (pH = ca. 9), and methanol. The solid was dissolved in hexafluoro-*i*-propanol, and the solution was passed through Celite®, and condensed. Reprecipitation in methanol gave a reddish powder, which was collected by filtration and dried under vacuum to obtain **(Taz(BOC)-Th-Th)$_n$-Pd** (0.74 g, 53% yield). ^{1}H NMR (300 MHz, DMSO-d_6) δ = 7.8–7.2 (br, 4H, thiophene-H), 1.6 and 1.2 (ca. 9H, —CH_3). IR (KBr, cm^{-1}): 1742 cm^{-1}, M_n = 10,800 M_w = 13,400.

The electrochemical oxidation of **monomer-7** (0.05 M) was conducted with Hokuto HVS-100 at a higher potential (e.g., 3.0 V vs. Ag$^+$/Ag) than the peak anodic potential of **monomer-7** (1.6 V vs. Ag$^+$/Ag). A 1 cm × 1 cm Pt plate, a 1 cm × 2 cm Pt plate, and BAS RE-5 0.1 M $AgNO_3$/Ag were used as the working electrode, counter electrode, and reference electrode, respectively, in an N_2-purged acetonitrile solution of $[Bu_4N]PF_6$ (Bu = butyl). Potentiostatic electrochemical polymerization at 3.0 V vs. Ag$^+$/Ag for 30 min gave a reddish-brown powder on the Pt working electrode. The powder was collected, washed with acetonitrile, and dried under vacuum at 60 °C. The dry powder was treated with an aqueous solution of hydrazine overnight, washed with water, and dried under vacuum at 60 °C to obtain a red-ocher product.

2.3.3. Treatment of polymers with acid

CF_3COOH (2 mL) was added to a suspension of the polymer sample (30 mg) in dichloromethane (2 mL) at room temperature. The mixture was stirred for 30 min at 60 °C and poured into 10 mL of water. After the removal of dichloromethane by evaporation at 60 °C, K_2CO_3 was added to neutralize the solution. The supernatant solution was decanted, and the precipitate was washed with methanol (20 mL). The powder was separated by centrifugation and dried under a reduced pressure.

3. Results and discussion

3.1. Preparation of *monomer-7* and related di-BOC compound, *compound B*

The reaction of 3,5-bis(2-thienyl)-4-amino-1,2,4-triazole (**compound A** [19,20]) with di-*t*-butyl dicarbonate, $(BOC)_2O$, in DMF gave the BOC-protected **monomer-7** (Scheme 5). By changing the solvent to THF, a related doubly BOC-protected species, **compound B**, was obtained.

Compound A showed a UV–Vis absorption peak at λ_{max} = 306 nm in DMF. This λ_{max} position was found at a longer wavelength than those of 1,2,4-triazole (216.5 nm [25]), thiophene (231 nm [25]), and 2,2′-bithiophene H-Th$_2$-H (302 nm [26]). The UV–Vis peak is located at a shorter wavelength than that of 2,2′:5′,5″-terthiophene H-Th$_3$-H (λ_{max} = 355 nm [26]), which has a coplanar molecular structure. However, the observed shift (Δ) in the UV–Vis absorption peaks from 1,2,4-triazole to **compound A** (Δ = approximately 13,500 cm^{-1}) is comparable to that observed for thiophene to H-Th$_3$-H (Δ = approximately 15,100 cm^{-1}). These UV–Vis data suggest that the π-conjugated system of 1,2,4-triazole extends across the thiophene–triazole–thiophene block, giving **compound A** a coplanar structure similar to that of H-Th$_3$-H. **Monomer-7** showed a λ_{max} at 307 nm, near that of **compound A**, indicating that the BOC substituent does not disturb the coplanar structure.

Fig. 1 shows the molecular structure of **monomer-7**. Crystallographic data of **monomer-7** are given in Table S1 in Supplementary information.

As shown in Fig. 1, the thiophene–triazole–thiophene block assumes an almost coplanar structure, supporting the discussion above. X-ray structural analysis indicated that **compound B** is also largely coplanar (cf. Supplementary information (SI)).

3.2. Poly(1-aminopyrrole-2,5-diyl)s, *P1-Ox* and *P1—Ni*, and their thermal treatment

The oxidative polymerization of **monomer-1** with $FeCl_3$ [11] gave **P1-Ox** (Scheme 2). The polymer was isolated after the treatment with methanol. Elemental analysis [11] and both IR and ^{1}H NMR spectroscopies supported the neutral polymer structure proposed for **P1-Ox**. **P1-Ox** was soluble in DMF and DMSO and partly soluble in chloroform; however, it was insoluble in hexane. GPC data indicated that **P1-Ox** had an M_n of 12,800 and an M_w of 17,600. The M_w corresponded to a degree of polymerization (DP) of 98. Fig. 2 shows the ^{1}H NMR spectrum of **P1-Ox**.

As shown in Fig. S1, a large ν(C=O) peak due to the BOC-protecting group of **P1-Ox** is observed at 1740 cm^{-1}. In the ^{1}H NMR spectrum, the pyrrole-H peaks are observed as broad signals. The presence of s-*cis* and s-*trans* rotamers, with respect to the conformation of the BOC-protecting group [11], accounts for the broadening of the signal.

The dehalogenative polycondensation of **monomer-2** with a zerovalent nickel complex (cf. Eq. (3) in Scheme 2) gave **P1—Ni**. The IR spectrum of **P1—Ni** was essentially the same as that of **P1-Ox** [11], despite its smaller M_n and M_w values (4,300 and 5,500 respectively). **P1—Ni** had better solubility in organic solvents than **P1-Ox** and was soluble in chloroform; however, it remained insoluble in hexane.

The thermal treatment of **P1** is expected to cause the deprotection of the —NH—BOC unit with the liberation of CO_2 and isobutene: $RNH\text{-}CO(OCMe_3) \rightarrow RNH_2 + CO_2 + CH_2 = CMe_2$ [13,14]. The IR spectra of the **P1**s thermally treated at 200 °C for 1 h showed the disappearance of the ν(C=O) peak at 1740 cm^{-1}. However, elemental analysis data deviated considerably from the calculated values for poly(1-amino-pyrrole-2,5-diyl) (cf. data shown below Fig. S2 in SI). The deprotected polymer may be unstable and susceptible to thermal decomposition. 1-aminopyrrole does not appear to have a high thermal stability as the suppliers recommended low-temperature storage [27]. The IR spectrum of thermally treated **P1-Ox** and the TGA data of **P1-Ox** are shown in Figs. S1 and S2.

.

3.3. Poly(aryleneethynylene)s (*PAE*s)

PAEs were prepared via Pd-catalyzed couplings of **monomer-3** and diethynyl compounds (cf. Scheme 3).

$$\textbf{monomer-3} + \textbf{monomer-4}\ (\text{or } \textbf{monomer-5}) \rightarrow \textbf{PAE-1}(\text{or } \textbf{PAE-2}) \quad (10)$$

GPC data showed that **PAE-1** and **PAE-2** had M_n values of 19,200 and 5,200 respectively, with poly-dispersities of 1.2 and 1.4 (eluent = chloroform and DMF for **PAE-1** and **PAE-2**, respectively; vs. polystyrene standards). **PAE-1** was soluble in THF, chloroform, and 1,2-dichlorobenzene, but was insoluble in dimethyl sulfoxide (DMSO), DMF, and hexafluoro-*i*-propanol (HFIP). **PAE-2** was soluble in DMSO, DMF, *N*-methyl-2-pyrrolidone (NMP), and HFIP, but was insoluble in chloroform and 1,2-dichlorobenzene. The IR spectra of **PAE-1** and **PAE-2** (cf. Fig. S3 in SI) were reasonable for the proposed molecular structures of the polymers and showed the BOC group ν(C=O) peak at approximately 1740 cm^{-1}. The ^{1}H NMR spectra of **PAE-1** and **PAE-2** were also reasonable (Fig. 3).

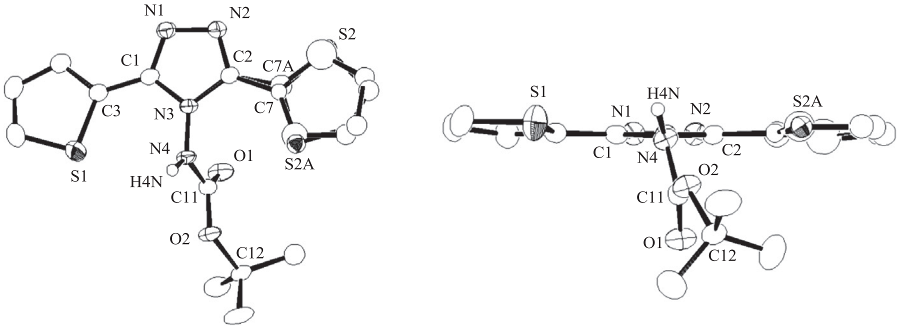

Fig. 1. Molecular structure of **monomer-7** (CCDC No.: 915788). The thiophene ring containing S2/S2A is disordered. Selected bond lengths and angles (Å, °): N1-N2 1.390(3), N1—C1 1.317(3), N2—C2 1.317(3), N3—C1 1.372(3), N3—C2 1.369(3), N3—N4 1.387(3), C1—C3 1.451(3), N4—C11 1.377(3), N4—H4N 0.860, N2—N1—C1 108.1(2), N1-—N2—C2 107.5(2), N1-—C1—N3 108.7(2), N2—C2—N3 109.3(2), C1—N3—C2 106.4(2), N3—N4—C11 116.1(2), N4—C11—O2 107.0(2), C11—O2—C12 120.5(2). Dihedral angles (°): triazole ring-thiophene ring containing S1 8.37(11), triazole ring-thiophene ring containing S2 8.06(11), triazole ring-thiophene ring containing S2A 6.6(2).

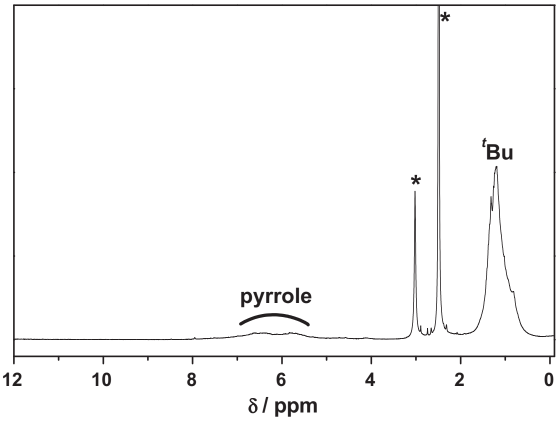

Fig. 2. ^{1}H NMR spectrum of **P1-Ox** in DMSO-d_6. Peaks with ∗ are due to solvent impurities (DMSO-d_5 and water).

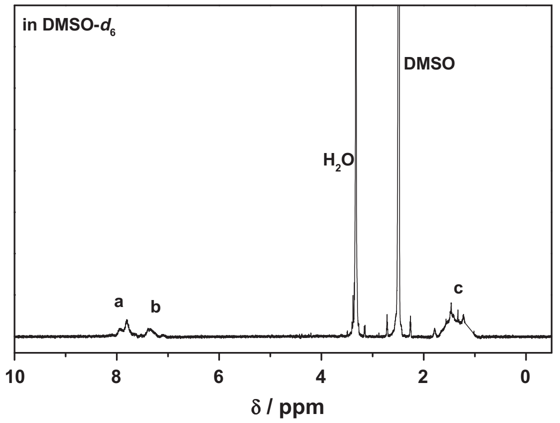

Fig. 3. ^{1}H NMR spectrum of **PAE-2** in DMSO-d_6. Additional peaks due to solvent impurities (DMSO-d_5, its spinning side bands, and H_2O) are also observed. ^{1}H NMR spectrum of **PAE-1** is shown in Fig. S4 in SI.

The peak area ratios in the ^{1}H NMR spectra of **PAE-1** and **PAE-2** were in rough agreement with a 1:1 ratio of **monomer-3** and diethynyl compounds (**monomer-4** and **monomer-5**) in the resultant polymers. However, the *C*/*N* molar ratio of **PAE-1** estimated from elemental analysis (*C*/*N* molar ratio = 13.6) somewhat deviated from the calculated molar ratio (*C*/*N* = 11.3), suggesting the presence of occasional Glaser coupling during the formation of **PAE**-type polymers [28,29].

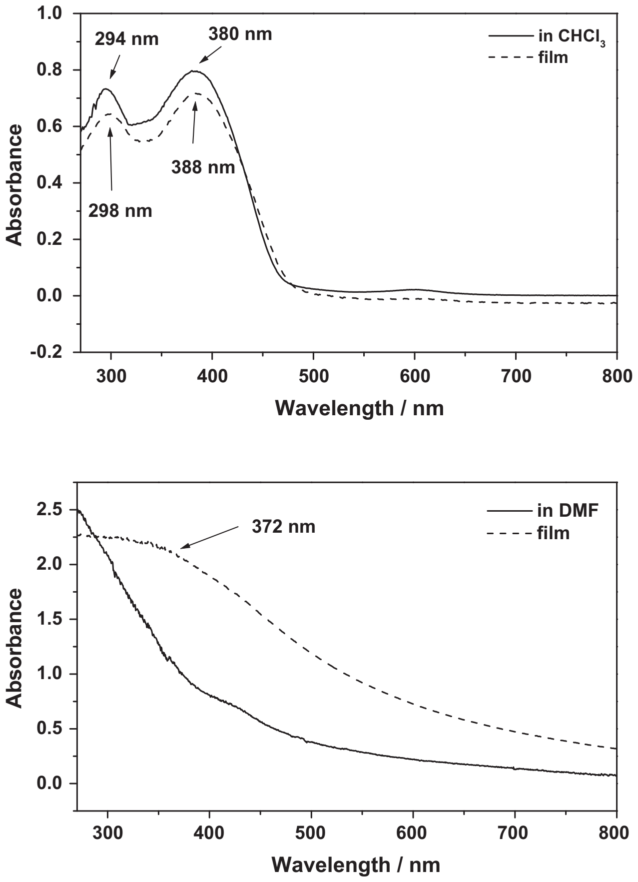

Fig. 4. UV–Vis spectra of (top) **PAE-1** and (bottom) **PAE-2** in solutions (chloroform for **PAE-1** and DMF for **PAE-2**: solid line) and films (dashed line). For the film samples, the absorbance is thought to contain contributions from the reflection on the surface of the film and partial scattering of light in the film.

Fig. 4 shows the UV–Vis spectra of **PAE-1** and **PAE-2** in solutions and films.

As shown in Fig. 4, the UV–Vis peak of **PAE-1** in chloroform appeared at 380 nm, which is strongly shifted to a longer wavelength (the shift Δ = ca. 20,000 cm^{-1}) than that of 1,2,4-triazole (216.5 nm [25]). In contrast, the UV–Vis spectrum of **PAE-2** in DMF showed no distinct peak in the range of 300–800 nm, due to the interruption of the conjugated π-system at the pyridine-2,6-diyl unit.

The UV–Vis spectrum of the solid-phase **PAE-1** film is similar to that in chloroform, suggesting the absence of intermolecular electronic interaction in the solid state. The UV–Vis spectrum of the **PAE-2** film shows a broad absorption band with a peak at approximately 370 nm. The appearance of the new absorption band might be due to the presence of intermolecular electronic interactions between **PAE-2** chains in the solid state.

Cast films of **PAE-1** and **PAE-2** on Pt plates showed two oxidation peaks at approximately 1.3 V and 1.6–1.8 V vs. Ag$^+$/Ag (Fig. S6 in SI). No CV peak was observed in the reduction region.

3.4. Bithiophene copolymers of 4-amino-1,2,4-triazole, *(Taz(BOC)$_2$-Th-Th)$_n$*

Reddish-ocher bithiophene copolymers of 4-amino-1,2,4-triazole were prepared via the Pd-catalyzed Stille-type polycondensation of **monomer-3** and **monomer-6** (cf. Scheme 3). The IR spectrum of the product (cf. Fig. S3 in SI) showed a ν(C=O) peak of the BOC group at 1756 cm^{-1}. **(Taz(BOC)-Th-Th)$_n$-Pd** was soluble in DMSO, NMP, and HFIP, somewhat soluble in DMF and THF, and insoluble in chloroform and 1,2-dichlorobenzene. Analysis of **(Taz(BOC)-Th-Th)$_n$-Pd** by GPC gave an M_n of 10,800 and an M_w of 13,400 (eluent = DMF; vs. polystyrene standards). Fig. S5 shows the ^{1}H NMR spectrum of **(Taz(BOC)-Th-Th)$_n$-Pd**. As shown in Fig. S5, thiophene-H signals (signals in region a) and BOC—H signals (signals in region b) appear at normal positions. The observation of two peaks in region b is attributed to the presence of the s-*cis* and s-*trans* rotamers of the BOC group [11]. The total peak area of the BOC—H signals is somewhat smaller than expected, suggesting partial deprotection (or BOC-removing reaction) during polymerization. The appearance of complicated thiophene-H ^{1}H NMR peaks may also be due to the presence of the s-*cis* and s-*trans* rotamers of the BOC group [11] and to partial deprotection during polymerization. The N*H* signals of the —NH—BOC group appear as a broad signal at approximately δ 11.5.

As shown in Fig. 5, the UV–Vis spectrum of **(Taz(BOC)-Th-Th)$_n$-Pd** shows a peak at 425 nm in DMF. The peak position in DMF (307 nm) was shifted to a longer wavelength by 118 nm (approximately 9,000 cm^{-1}) compared with those in the trimeric compounds, **compound A** and **monomer-7**, due to the expansion of the π-conjugation length in **(Taz(BOC)-Th-Th)$_n$-Pd**.

The λ_{max} of **(Taz(BOC)-Th-Th)$_n$-Pd** is comparable to that of polythiophenes (approximately 450 nm [24,26]), which are typical π-conjugated five-membered ring polymers. The **(Taz(BOC)-Th-Th)$_n$-Pd** film displays a UV–Vis peak at essentially the same position as that in DMF solution, suggesting that there is no significant intermolecular electronic interaction between polymer molecules in the solid state.

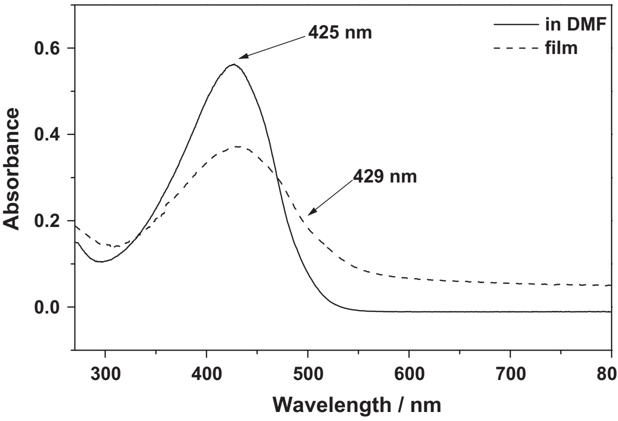

Fig. 5. UV–Vis spectra of **(Taz(BOC)-Th-Th)$_n$-Pd** in DMF (solid line) and cast film (dashed line). For the film sample, the absorbance is thought to contain contributions from the reflection on the surface of the film and partial scattering of light in the film.

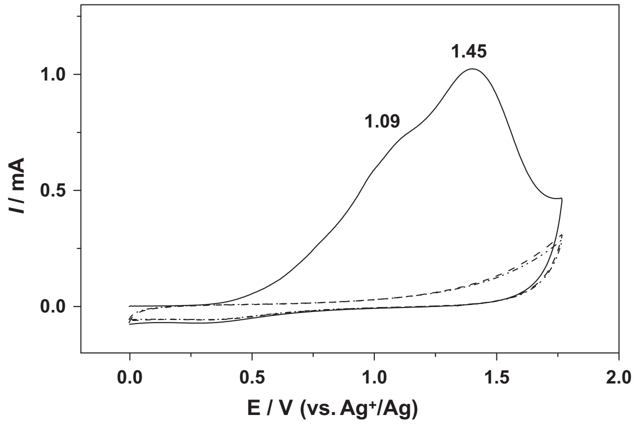

Fig. 6. CV charts of **(Taz(BOC)-Th-Th)$_n$-Pd** (cast film on a Pt plate) in 1st (solid line), 2nd (dashed line), and 3rd scans. In an acetonitrile solution of 0.10 M [NBu$_4$]PF$_6$ (Bu = butyl).

As shown in Fig. 6, **(Taz(BOC)-Th-Th)$_n$-Pd** undergoes a two-step electrochemical oxidation with peak current anodic potentials (E_{pa}s) of 1.09 V and 1.45 V vs. Ag$^+$/Ag.

The E_{pa}s of **(Taz(BOC)-Th-Th)$_n$-Pd** are at considerably higher potentials than those (0.5–0.7 V vs. Ag$^+$/Ag) of poly(thiophene-2,5-diyl) and poly(3-alkylthiophene-2,5-diyl) [26,30,31] indicating that the 4-amino-1,2,4-triazole unit is an electron-accepting unit due to the presence of electron-withdrawing imine —C=N— groups.

Electron-accepting π-conjugated polymers usually show electrochemical reduction peaks in their CV scans. However, no such electrochemical reduction peak was observed for **(Taz(BOC)-Th-Th)$_n$-Pd**. The electrochemical oxidation was irreversible (Fig. 6). The de-doping peak was not clearly observed, and the oxidation peaks became very weak in the 2nd cycle. This result suggests that the PF$_6^-$ dopant incorporated into the polymer film in the first cycle is trapped by the oxidized, positively charged **(Taz(BOC)-Th-Th)$_n$-Pd** and does not separate from the polymer film in the reverse scan. π-Conjugated polymers sometimes give irreversible CV peaks when they have coordinating elements, such as oxygen in alkoxy groups, and/or the anion dopant is large [31,32] presumably due to the trapping of the anion dopant by the polymers.

The electrochemical polymerization of **monomer-7** was conducted using a Pt plate as a working electrode in an acetonitrile solution of 0.10 M [NBu$_4$]PF$_6$ (Scheme 4). The CV of **monomer-7** (cf. Fig. S7 in SI) showed an oxidation peak (peak current anodic potential) at E_{pa} = 1.36 V vs. Ag$^+$/Ag, which is a higher potential than that of terthiophene (E_{pa} = 0.97 V [26,33] vs. SCE (−0.34 V vs. Ag$^+$/Ag [34–37]), due to the electron-withdrawing nature of the central 1,2,4-triazole unit. The potentiostatic electrochemical polymerization of **monomer-7** (0.05 M in acetonitrile) at 3.0 V vs. Ag$^+$/Ag (electrolyte = 0.10 M [NBu$_4$]PF$_6$) gave a reddish-ocher powder on the Pt plate electrode. No formation of such a reddish ocher powder was observed below the oxidation potential (e.g., at 2.8 V vs. Ag$^+$/Ag).

The presence of a PF$_6^-$ peak at 848 cm^{-1} in its IR spectrum (cf. Fig. S8 in SI) suggested that the polymer is formed in a p-doped state. The reduction of the polymer with N$_2$H$_4$ gave a PF$_6^-$-dopant-free polymer, as judged by the disappearance of the PF$_6^-$ IR peak. Treatment with N$_2$H$_4$ also resulted in the loss of the BOC-protecting group, as evidenced by the disappearance of the ν(C=O) IR peak (Fig. S8). This PF$_6^-$-doped polymer (**(Taz(BOC)-Th-Th)$_n$-Ox**) had better solubility than **(Taz(BOC)-Th-Th)$_n$-Pd**, presumably due to its lower molecular weight. It was soluble in DMSO, DMF,

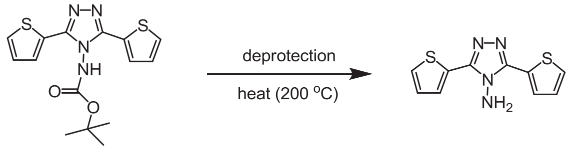

monomer-7 **compound A** (11)

Scheme 6. Thermal BOC-deprotection of **monomer-7** to produce **compound A** (cf. Scheme 5).

THF, and HFIP, but insoluble in chloroform. GPC analysis of **(Taz(BOC)-Th-Th)$_n$-Ox** in DMF gave M_n and M_w values of 4,200 and 5,800 respectively. The ^{1}H NMR spectrum of **(Taz(BOC)-Th-Th)$_n$-Ox** shows a complex peak pattern, suggesting both the α,α′-coupling and α,β-coupling at the thiophene ring. The occurrence of α,β-coupling, in addition to α,α′-coupling, in the electrochemical polymerization of thiophene has been reported [38]. On the basis of these results, organometallic polycondensation (Eq. (6)) is superior to electrochemical polymerization (Eq. (7)) for the preparation of **(Taz(BOC)-Th-Th)$_n$**.

3.5. Deprotection of BOC group in BOC-protected 4-amino-1,2,4-triazole polymers such as *(Taz(BOC)$_2$-Th-Th)$_n$-Pd*

All of the BOC-protected 4-amino-1,2,4-triazole polymers (**PAE-1**, **PAE-2**, and **(Taz(BOC)-Th-Th)$_n$-Pd**, shown in Scheme 3) underwent the thermal deprotection of the BOC group at 200 °C. The ν(C=O) peak of the BOC group disappeared or became much smaller in the thermally treated polymers. After the deprotection of the BOC group, the polymers became insoluble in organic solvents [39]. Multiple interpolymer hydrogen bonds between the —NH$_2$ group and the —N=N— units at the 1,2-positions are formed [40] when the BOC group is removed, causing the insolubility of the deprotected polymers in solvents. Changes in the IR spectra of **PAE-1** and **PAE-2** caused by the thermal deprotection are shown in Figs. S9 and S10a. The ^{13}C-CP/MAS NMR spectrum of thermally BOC-deprotected **PAE-2** is shown in Fig. S11 in SI.

The deprotection of BOC-protected organic amines can also be conducted by treatment with acids such as CF$_3$COOH [41–43]. The treatment of **PAE-2** with CF$_3$COOH (cf. experimental section) gave a sample without a ν(C=O) peak in the IR spectrum, indicating successful deprotection (cf. Fig. S10b in SI).

The thermal BOC-deprotection of **monomer-7** shown in Scheme 6 was examined by TGA and ^{1}H NMR spectroscopy.

Fig. S12 shows the TGA curve for **monomer-7**. The deprotection of the BOC-group started at approximately 190 °C (Fig. S12) and resulted in a 28% weight loss, in agreement with the calculated theoretical weight loss for deprotection (28.7%).

Fig. 7 shows a comparison of the ^{1}H NMR spectra of **compound A** synthesized according to the literature (cf. experimental part [19,20]), **monomer-7**, and the product obtained after the thermal BOC-deprotection of **monomer-7**.

As shown in Fig. 7, the BOC-CH$_3$ peak of **monomer-7** disappeared after thermal treatment, and the ^{1}H NMR spectrum of the product is in agreement with that of **compound A**. These results (Figs. 7 and S12), in conjunction with the IR data, indicate that the thermal BOC-deprotection was effective.

Fig. S13a shows the changes in the IR spectrum of **(Taz(BOC)-Th-Th)$_n$-Pd** with thermal BOC-deprotection at 200 °C. As shown in Fig. S13a, the strong ν(C=O) band of the BOC group at 1742 cm^{-1} disappeared after thermal BOC-deprotection.

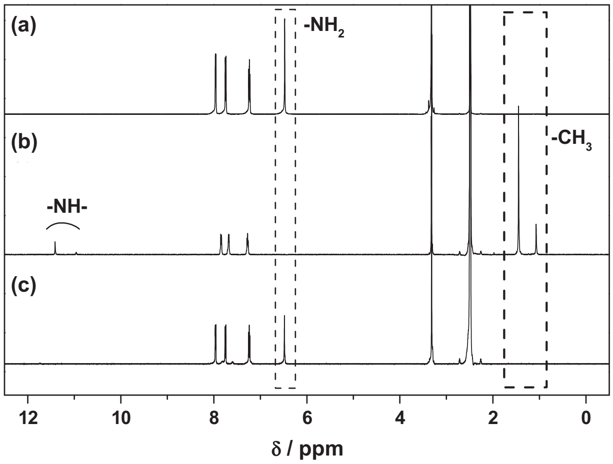

Fig. 7. ^{1}H NMR spectra of (a) **compound A**, (b) **monomer-7**, and (c) the product obtained after the thermal BOC-deprotection of **monomer-7** in DMSO-d_6. The presence of both the s-*cis*- and s-*trans* rotamers [11] of **monomer-7** resulted in two peaks for each of the NH and CH$_3$ groups. The large peaks at δ 2.6 and 3.4 ppm are due to the DMSO-d_6 impurity and H$_2$O, respectively (cf. Fig. S5).

The ^{13}C-CP/MAS NMR spectrum of the thermally BOC-deprotected polymer, **(Taz-Th-Th)$_n$-Pd**, is shown in Fig. S14. As shown in Fig. S14, the ^{13}C-CP/MAS NMR spectrum of **(Taz-Th-Th)$_n$-Pd** shows two peaks at δ 125.7 and 136.3 ppm. The peak positions are comparable with those of poly(thiophene-2,5-diyl) (δ 125.7 and 136.5 ppm) and are assigned to the 3,4- and 2,5-carbons of the Th unit [44,45]. Because the ^{13}C NMR signal of the 3,5-C of 4-amino-1,2,4-triazole appears at a lower filed (by approximately 20 ppm) than that of thiophene [46], the δ 150.7 ppm signal of **(Taz-Th-Th)$_n$-Pd** is assigned to the 3,5-C of the 4-amino-1,2,4-triazole unit. **(Taz(BOC)-Th-Th)$_n$-Pd** also undergoes CF$_3$COOH-induced BOC-deprotection, as indicated by the disappearance of the ν(C=O) IR peak after the treatment with CF$_3$COOH (cf. Fig. S13b in SI).

Although the BOC-deprotected polymer, **(Taz-Th-Th)$_n$-Pd**, is insoluble in solvents, as described above, its UV–Vis and CV data can be obtained using a **(Taz-Th-Th)$_n$-Pd** film obtained by the thermal treatment of a cast film of **(Taz(BOC)-Th-Th)$_n$-Pd**. The UV–Vis absorption peak of the **(Taz-Th-Th)$_n$-Pd** film shifted to a somewhat longer wavelength than that of **(Taz(BOC)-Th-Th)$_n$-Pd** (Fig. S15). The tailing off of the UV–Vis absorption band of **(Taz-Th-Th)$_n$-Pd** suggests the presence of intermolecular electronic interaction in the solid state. **(Taz-Th-Th)$_n$-Pd** showed similar CV behavior to **(Taz(BOC)-Th-Th)$_n$-Pd** (cf. Fig. 6); the CV of the **(Taz-Th-Th)$_n$-Pd** film is shown in Fig. S16.

As described above, the BOC-group protected π-conjugated polymers consisting of 4-amino-1,2,4-triazole units (**PAE-1**, **PAE-2**, and **(Taz(BOC)-Th-Th)$_n$-Pd**) have been prepared by Pd-catalyzed polycondensation. These polymers are thought to have essentially coplanar structures. Because of the solubilizing effect of the BOC group, the optical and electrochemical properties of the polymers could be measured. Thermal BOC-deprotection proceeds cleanly to yield the coplanar **(Taz-Th-Th)$_n$-Pd** polymer.

Acknowledgements

We are grateful to Mr. Hiroyasu Sato and Mr. Takashi Takasaki of Rigaku Corporation for the crystallographic analysis of **compound B**. Thanks are also due to Professor Y. Nakamura and Dr. M. Abe of our laboratory for experimental support and helpful discussion.

Appendix A. Supplementary material

Supplementary data associated with this article can be found, in the online version, at http://dx.doi.org/10.1016/j.reactfunctpolym.2013.05.013.

References

[1] T.A. Skotheim, J.R. Reynolds (Eds.), Handbook of Conducting Polymers, third ed., CRC Press, Boca Raton, Florida, 2007.

[2] H.S. Nalwa (Ed.), Handbook of Organic Conductive Molecules and Polymers, John Wiley, Chichester, 1997.

[3] P.-C. Wang, J.-Y. Yu, React. Funct. Polym. 72 (2012) 311–316.

[4] A. Kivrak, B.B. Carbas, M. Zora, A.M. Önal, React. Funct. Polym. 72 (2012) 613–620.

[5] L. Liu, F. Tian, X. Wang, Z. Yang, M. Zhou, X. Wang, Funct. Polym. 72 (2012) 45–49.

[6] H. Wu, B. Qu, Z. Cong, H. Liu, D. Tian, B. Tian, B. Gao, Z. An, C. Gao, L. Xiao, Z. Chen, H. Liu, Q. Gong, W. Wei, React. Funct. Polym. 72 (2012) 897–903.

[7] T. Yamamoto, N. Hayashida, React. Funct. Polym. 37 (1998) 1–17.

[8] J. Losada, M.P.G. Armada, Electroanalytical 13 (2001) 1016–1021.

[9] T. Kuwahara, N. Yamakawa, T. Momma, T. Osaka, Electrochemistry (Tokyo) 69 (2001) 598–602 (Chem. Abstr. 135 (2001) 186811).

[10] Y. Murakami, T. Yamamoto, Polym. J. 31 (1999) 476–478.

[11] T. Yamamoto, G. Tanaka, H. Fukumoto, T.-A. Koizumi, Heterocycles 78 (2009) 117–125.

[12] I. Yamaguchi, T. Asano, J. Mater. Sci. 46 (2011) 4582–4587.

[13] J.P. Sadighi, R.A. Singer, S.L. Buchwald, J. Am. Chem. Soc. 120 (1998) 4960–4976.

[14] X.-X. Zhang, J.P. Sadighi, T.W. Mackewitz, S.L. Buchwald, J. Am. Chem. Soc. 122 (2000) 7606–7607.

[15] T. Yamamoto, M. Yoshizawa, A. Mahmut, M. Abe, S.-I. Kuroda, T. Imase, S. Sasaki, J. Polym. Sci. Part A: Polym. Chem. 43 (2005) 6223–6232.

[16] Y. Suwa, R. Arita, K. Kuroki, H. Aoki, J. Surface Sci. Nanotechnol. 2 (2004) 38–44.

[17] R. Arita, Y. Suwa, K. Kuroki, H. Aoki, Kotai Butsuri 40 (2005) 177–187 (Chem. Abstr. 142 (2005) 392873).

[18] Y.-M. Tang, Y. Chen, W.-Z. Yang, Y. Liu, X.-S. Yin, J.-T. Wang, J. Appl. Electrochem. 38 (2008) 1553–1559.

[19] F. Bentis, M. Lagrenée, M. Traisnel, B. Mernari, H. Elattari, J. Heterocycl. Chem. 36 (1999) 149–152.

[20] Y. Ikemi, N. Hayashi, A. Kakehi, K. Matsumoto, Heterocycl. Commun. 8 (2002) 439–442.

[21] T. Morikita, T. Yasuda, T. Yamamoto, Reactive Funct. Polym. 68 (2008) 1483–1491.

[22] C. Weder (Ed.), Poly(aryleneethynylene)s, Springer, Berlin, 2005.

[23] T. Yamamoto, K. Honda, N. Ooba, S. Tomaru, Macromolecules 31 (1998) 7–14.

[24] T. Yamamoto, Bull. Chem. Soc. Jpn. 83 (2010) 431–455.

[25] R.C. Weast, CRC Handbook of Chemistry and Physics, 58th ed., CRC Press, Cleveland, Ohio, 1977.

[26] D. Fichou (Ed.), Handbook of Oligo- and Polythiophene, Wiley-VCH, Weinheim, 1999.

[27] Supplier: Tokyo Chemical Industry Co., Ltd. Data for 1-aminopyrrole can be obtained from internet.

[28] T. Mangel, A. Eberhardt, U. Scherf, U.H.F. Bunz, K. Müllen, Macromol. Rapid Commun. 16 (1995) 571–580.

[29] H. Fukumoto, K. Yamane, Y. Kase, T. Yamamoto, Macromolecules 43 (2010) 10366–10375.

[30] T. Yamamoto, H. Kokubo, Electrochim. Acta 50 (2005) 1453–1460.

[31] T. Yamamoto, A. Morita, Y. Miyazaki, T. Maruyama, H. Wakayama, Z.-H. Zhou, Y. Nakamura, T. Kanbara, S. Sasaki, K. Kubota, Macromolecules 25 (1992) 1214–1223.

[32] T. Yamamoto, Q. Fang, T. Morikita, Macromolecules 36 (2003) 4262–4267.

[33] E.E. Havinga, L.W. van Horssen, Makromol. Chem. Makromol. Symp. 24 (1989) 67–76.

[34] R. Tomot, S. Zecchin, G. Schiavon, G. Zotti, J. Electroanal. Chem. Interfacial Electrochem. 252 (1988) 215–219.

[35] G. Schiavon, G. Zotti, G. Bontempelli, J. Electroanal. Chem. Interfacial Electrochem. 194 (1985) 327–338.

[36] G. Schiavon, G. Zotti, G. Bontempelli, J. Electroanal. Chem. Interfacial Electrochem. 161 (1984) 323–335.

[37] The Epa of monomer-7 (0.97 V vs. SCE) is calculated as 0.63 V vs. Ag^+/Ag using the relation between SCE and Ag^+/Ag.

[38] K. Tanaka, T. Shichiri, T. Yamabe, Synth. Met. 16 (1986) 207–214.

[39] Thermally treated **PAE-1** was partly soluble in 1,2-dichlorobenzene at 130 °C.

[40] For example Y.-W. Zhang, J.-Q. Wang, L. Cheng, Acta Cryst. E65 (2009) o2261.

[41] N. Srinivasan, A. Yurek-George, A. Ganesan, Mol. Divers. 9 (2005) 291–293.

[42] I.W. Ashworth, B.G. Cox, B. Meyrick, J. Org. Chem. 75 (2010) 8117–8125.

[43] P. Palladino, D.A. Stetsenko, Org. Lett. 14 (2012) 6346–6349.

[44] T. Yamamoto, T. Kamijoh, I. Wataru, J. Polym. Sci.: Part A: Polym. Chem. 38 (2000) 1642–1646.

[45] S. Hotta, T. Hosaka, M. Soga, W. Shimotsuma, Synth. Met. 10 (1984) 95–99.

[46] Data base of AIST (National Institute of Advanced Industrial Science and Technology).